World Applied Sciences Journal 34 (1): 109-119, 2016
ISSN 1818-4952

DOI: 10.5829/idosi.wasj.2016.34.1.420

Threshold Acceleration for the Onset of Permanent Seismic Deformation of Sand Slopes

Mohamed F. Mansour

Ain Shams University, Cairo, Egypt

Abstract: Newmark's sliding block model accounts for the permanent seismic deformation of slopes only when the factor of safety drops below unity. Numerical analysis shows, however, that permanent seismic deformations accumulate at higher safety factors. In this paper, new threshold acceleration is defined for dry sand slopes such that the permanent seismic deformation from Newmark-type analysis matches the output of seismic finite element analysis. The proposed threshold acceleration marks the onset of permanent seismic deformation development inside the soil mass and, hence, is lower than Newmark's yield acceleration required for the development of a complete failure surface. Different slope heights, surface surcharges and input motion intensities are investigated. The results show that the proposed threshold acceleration corresponds to 83-96% of the static factor of safety. The deduced range can be used to estimate lower and upper bounds of the permanent seismic deformation. The threshold acceleration is correlated with the peak crest acceleration through a power function.

Key words: Newmark's sliding block model · Permanent seismic deformation · Seismic finite element analysis · Threshold acceleration

INTRODUCTION

Newmark [1] developed the sliding block model to calculate the permanent seismic deformation of infinite slopes. Newmark considered that permanent seismic deformation occurs only when the factor of safety drops below unity. The "yield acceleration" of the slope was defined as the acceleration corresponding to a factor of safety of unity. Accelerations in excess of the yield acceleration are double integrated to calculate the permanent seismic slope deformation. Chopra [2] extended Newmark's work in order to calculate the permanent seismic deformation of finite slopes. Using dynamic numerical analysis, Chopra integrated the horizontal components of the dynamic shear stresses over the potential sliding wedge at each time step during the seismic excitation. The "average acceleration" was defined as the total horizontal seismic shear force divided by the mass of the potential sliding wedge. The average acceleration at each time step during the seismic excitation is used to run a limit equilibrium analysis and, hence, the corresponding factor of safety is calculated. The yield acceleration is the average acceleration corresponding to a factor of safety of unity.

Elgamal *et al.* [3] used a simple sliding-block model to simulate the recorded deformations of the La Villita Dam in Mexico from five strong earthquakes. They found that a limit equilibrium analysis of the most-critical sliding surface might not be useful to account for the slope deformation, because it does not account for the existence of local weak zones, which attract high deformations because of their small yield accelerations. Mateo [4] performed two-dimensional dynamic finite element analyses and Newmark-type sliding block analysis to investigate the seismic behavior of the Patillas Earth Dam. The yield acceleration was defined as the acceleration corresponding to a factor of safety of unity. Du [5] proposed a new one-step Newmark displacement model based on seismological variables like the moment magnitude and rupture distance rather than intensity measures. The modified Newmark model by Du [5] yielded better prediction of the slope displacements. Zangeneh [6]

Corresponding Author: Mohamed F. Mansour, El Sarayat Street, Abassia, Cairo, Egypt, 11517.
Cell: +20 109 981 5877.

proposed enhancements to Newmark sliding block model to account for the seismically induced excess pore water pressure during the earthquake and its dissipation after the end of the earthquake. Wartman [7] compared the results of Newmark-type analysis with the results of physical model tests and found that Newmark-type analysis provides about 40-85% of the maximum measured displacements in the physical models.

Some studies (Law *et al.* [8], Finn *et al.* [9], USBR [10] and Kourkoulis *et al.* [11]) revealed that the permanent seismic deformation of slopes occurs when the shear stresses induced during the seismic excitation exceeds the available static shear strength of the soil, in absence of liquefaction. Therefore, the permanent seismic deformation of a slope can be obtained by first calculating the seismic shear stresses using a numerical technique (finite element or finite difference) and then performing a post-earthquake static deformation analysis to compare the seismic shear stresses with the available static shear strength.

Newmark model and Chopra modifications are implemented in the finite element/limit equilibrium software Geostudio 2007 ([12], [13] and [14]) to estimate the permanent seismic deformation of finite slopes. At each time step during the earthquake, the seismic shear stresses resulting from the seismic finite element analysis are integrated to calculate the "average acceleration". Subsequent limit equilibrium analyses are conducted to obtain the corresponding factor of safety. Accelerations in excess of the yield acceleration are double integrated to calculate the permanent seismic slope deformation (limit equilibrium approach). The seismic shear stresses can be also used as input into static finite element analyses at each time step to calculate the permanent seismic deformation (numerical approach).

The numerical analysis approach is more rigorous than Newmark/Chopra approach with its present definition of the yield acceleration. In many cases, it is found that Newmark/Chopra approach yields zero permanent seismic deformation, because the average acceleration corresponds always to a factor of safety more than unity. On the other side, the numerical approach accumulates plastic deformation, if any, at every single node of the finite element or finite difference mesh. The main disadvantage of Newmark/Chopra approach is the assumption of the occurrence of permanent seismic deformation only when the factor of safety drops below unity.

In this paper, a new threshold acceleration for finite sand slopes is proposed such that the permanent seismic deformation calculated using Newmark/Chopra approach matches the value calculated using the numerical approach. The proposed threshold acceleration marks the onset of permanent seismic deformation development inside the soil not the development of a complete failure surface. The proposed threshold acceleration provides a practical match between Newmark/Chopra approach and the numerical approach.

Problem Configuration: The investigated slopes are composed of dry sand with heights ranging from 3.0 to 5.0 meters. Dry slopes only are investigated to exclude the effect of seismically induced pore water pressures on the shear strength drop and, hence, the permanent seismic deformation. The side slopes are taken 2H: 1V. Uniform surcharges ranging from 20 kPa to 200 kPa are applied on the top of the slope. The surcharge load extends from the crest to a distance of 10.0 m from the crest. The lower boundary is taken at a depth of 10.0 m below the slope toe. Preliminary analyses have shown that the free field conditions can be reproduced with the left and right boundaries at 30.0 m from the toe and from the end of the surcharge load. Figure 1 shows a typical geometrical configuration of the problem. Table 1 summarizes the investigated cases.

Materials Properties: The problem of the permanent seismic deformation of slopes subjected to seismic excitation is important when the serviceability is a design concern. A footing resting on a slope is an example of this class of problems. Therefore, it is considered that the dry sand is in a dense to very dense condition and the internal friction angle is taken 36°. The secant modulus at 50% of the failure stress (E_{50}) is varied with the confining stress according to Equation (1).

$$E_{50} = E_{ref} \cdot \left(\frac{\sigma'_3}{p_{ref}} \right)^m \tag{1}$$

where σ'_3 is the effective confining pressure, which equals the at rest earth pressure coefficient (K_o) times the effective vertical stress (σ'_v), p_{ref} is the reference pressure, taken 100 kPa, m is a stress exponent and equals 0.5 for cohesionless soils (Janbu [15]) and E_{ref} is the modulus corresponding to the reference pressure, taken 100 Mpa.

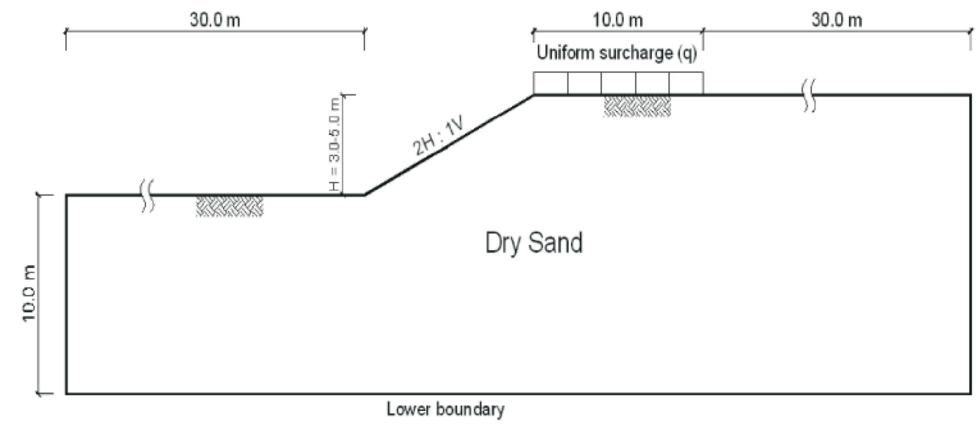

Fig. 1: Typical geometrical configuration of the studied slopes

Table 1: Main attributes of the investigated slopes

Case ID	Slope height (m)	Applied surcharge (kPa)
1	5.0	20.0
2	5.0	40.0
3	5.0	50.0
4	5.0	60.0
5	5.0	120.0
6	5.0	150.0
7	5.0	200.0
8	4.0	120.0
9	4.0	200.0
10	3.0	120.0
11	3.0	200.0

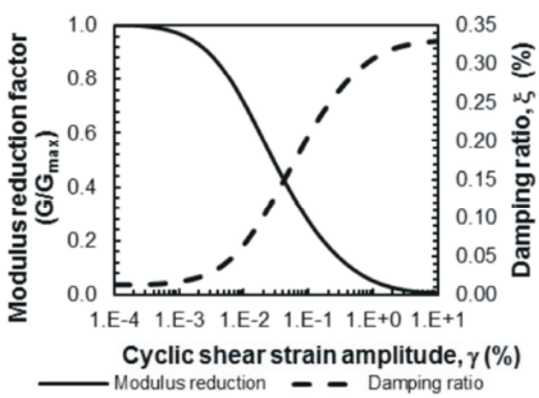

Fig. 2: Variations of the modulus reduction factor (G/G_{max}) and damping ratio (ξ) with the cyclic shear strain amplitude (γ)

Equation (2) by Seed and Idriss [16] is used to calculate the maximum shear modulus as a function of the mean principal stress.

$$G_{\max} = 1000 * K_{2,\max} * (\sigma'_m)^{0.5} \quad [2]$$

where G_{max} is the maximum shear modulus in units of lb/ft^2, $K_{2,\,max}$ is a unitless factor that depends on the value of the relative density and σ'_m is the mean principal stress ($\frac{\sigma'_v + 2 * K_0 * \sigma'_v}{3}$) in lb/ft^2. The value of $K_{2,\,max}$ is taken 59 ($D_r \geq 75\%$).

The variations of the modulus reduction factor (G/G_{max}) and damping ratio (ξ) with the cyclic shear strain amplitude (γ) are estimated according to the correlations developed by Ishibashi and Zhang [17] and are illustrated in Figure 2.

Input Motion: An artificial earthquake time history is utilized to define the input motion at the lower boundary, based on the standard response spectrum of the Uniform Building Code (Abdel-Motaal [18]). Figure 3 shows the input time history for a peak horizontal acceleration of 0.07g. Additional analyses are conducted with peak base accelerations of 0.10g, 0.125g, 0.15g and 0.175g. Mokhtar *et al*. [19] concluded that the lateral seismic displacement of piles in liquefiable soils is slightly affected when the earthquake duration increases from 20 to 40 seconds. Hence, the earthquake duration is taken 20 seconds in the conducted analyses.

Analysis Results

Permanent Seismic Deformation Using the Finite Element Method: Static finite element analyses are conducted to establish the static stresses due to the soil own weight and the applied surcharge. Mohr-Coulomb failure criterion is used to define the yield conditions; i.e. the constitutive law is elastic-perfectly plastic under static conditions. Figure 4 shows a typical finite element mesh used in the static analyses. The triangular elements are chosen with a size of 0.5m in the slope zone. The mesh gets coarser towards the lower and side boundaries.

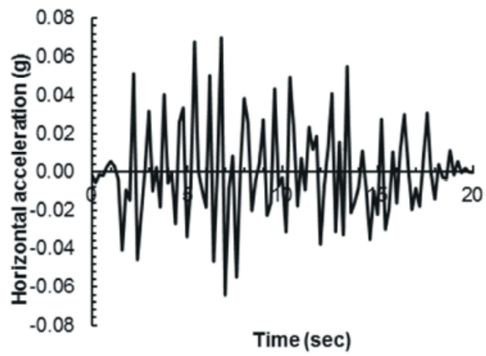

Fig. 3: Input motion time history

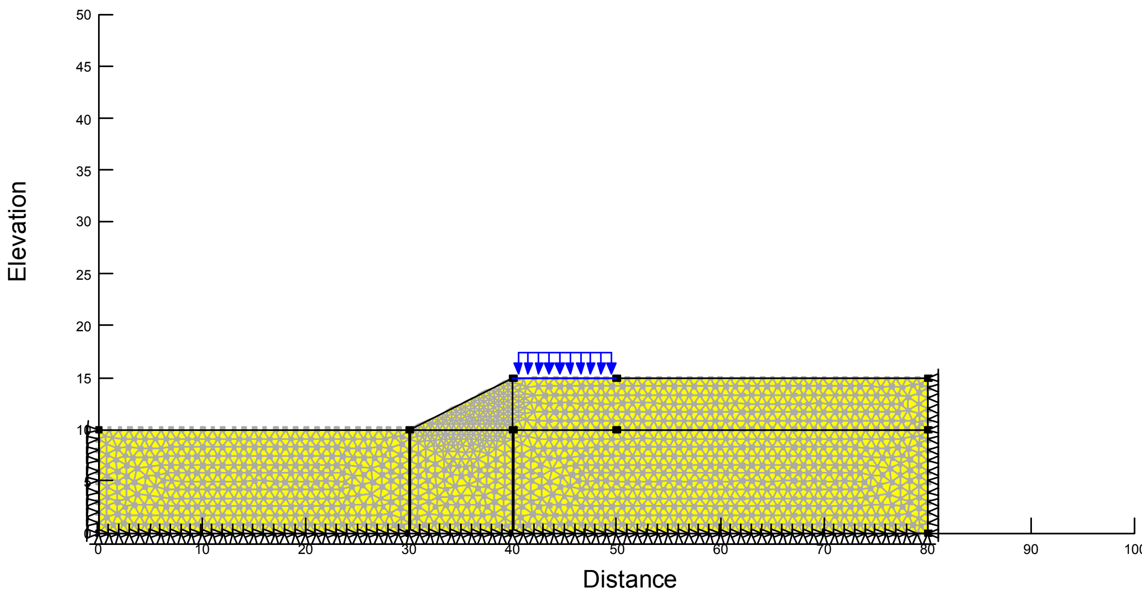

Fig. 4: Typical finite element mesh in static analyses

The seismic analyses are conducted mainly using a peak base acceleration of 0.07g. The effect of varying the peak base acceleration is illustrated for some cases. The finite element mesh in the seismic analyses is similar to the static mesh except for the side boundaries, which are restrained in the vertical direction only to ensure that the earthquake waves are not radiated back into the investigated domain. The Equivalent Linear Model is used to define the degradation of the soil shear modulus with the cyclic shear strain amplitude. The aim of the seismic analysis is to determine the seismic shear stresses, which will be compared with the static shear strength to calculate the permanent seismic deformation. Therefore, it is considered that there is no need to adopt a sophisticated nonlinear dynamic model.

The seismic shear stresses are calculated every 0.2 seconds approximately during the earthquake. At each time step, a subsequent static finite element analysis compares the seismic shear stress at each node with the available shear strength. If the static shear strength is exceeded, permanent seismic deformation is calculated.

Figure 5 shows, for a slope height of 5.0 m and a peak base acceleration of 0.07g, the resultant permanent seismic deformation at the end of the earthquake along a line extending from the crest to fifteen meters away, i.e. until 5.0 m from the end of the applied surcharge. The peak crest acceleration is also shown. The shown deformation is the resultant of the absolute horizontal and vertical deformations. The permanent seismic deformation is always in the downslope direction. The permanent seismic deformation time history at the toe is found negligible relative to the crest deformation. Figure 6 shows the shape of the deformed mesh for the case of a 5m-high slope loaded with a surcharge of 120 kPa (peak base acceleration = 0.07g).

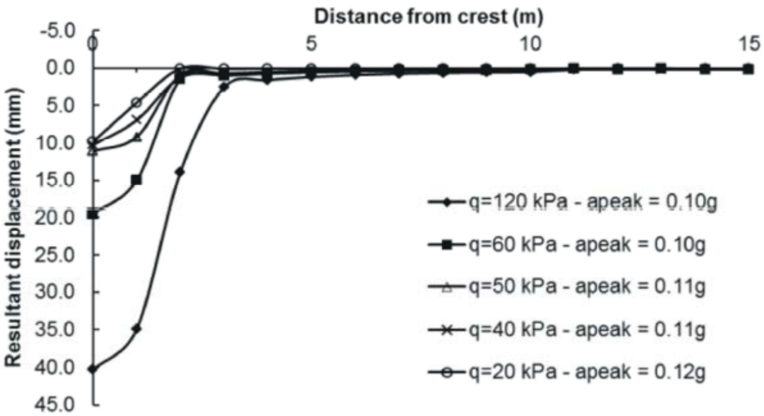

Fig. 5: Resultant permanent seismic deformation at the slope crest for a slope height of 5m and peak base acceleration of 0.07g

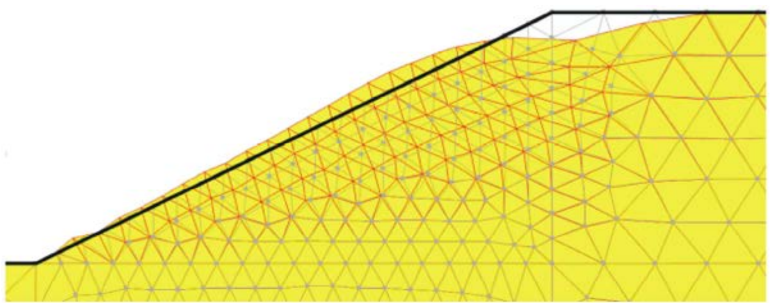

Fig. 6: Deformed mesh of the 5m-high slope loaded with surcharge q=120 kPa, 20X (peak base acceleration = 0.07g)

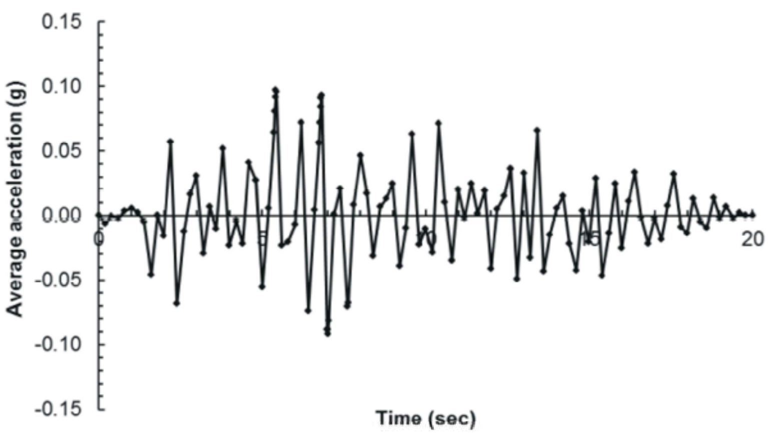

Fig. 7: Average acceleration time history of the 5m-high slope loaded with 120 kPa (peak base acceleration = 0.07g)

Threshold Acceleration: According to Newmark model [1] and Chopra [2] modifications, a limit equilibrium analysis is conducted at each time step during the seismic excitation. The factor of safety corresponding to the average acceleration at each time step is calculated. Hence, a relationship between the factor of safety and the average acceleration can be established. Figure 7 shows the average acceleration time history for the 5m-high slope loaded with 120 kPa and Figure 8 shows the factor of safety versus the average acceleration for all the studied slopes at a peak base acceleration of 0.07g. Figures 7 and 8 show that the factor of safety never drops below unity and, hence, the permanent seismic deformation equals zero according to Newmark's definition of the yield acceleration.

The factor of safety at an average acceleration of zero is the static factor of safety, by definition. Figure 8 shows that the factor of safety is lower than the static value when the average acceleration is positive and vice versa.

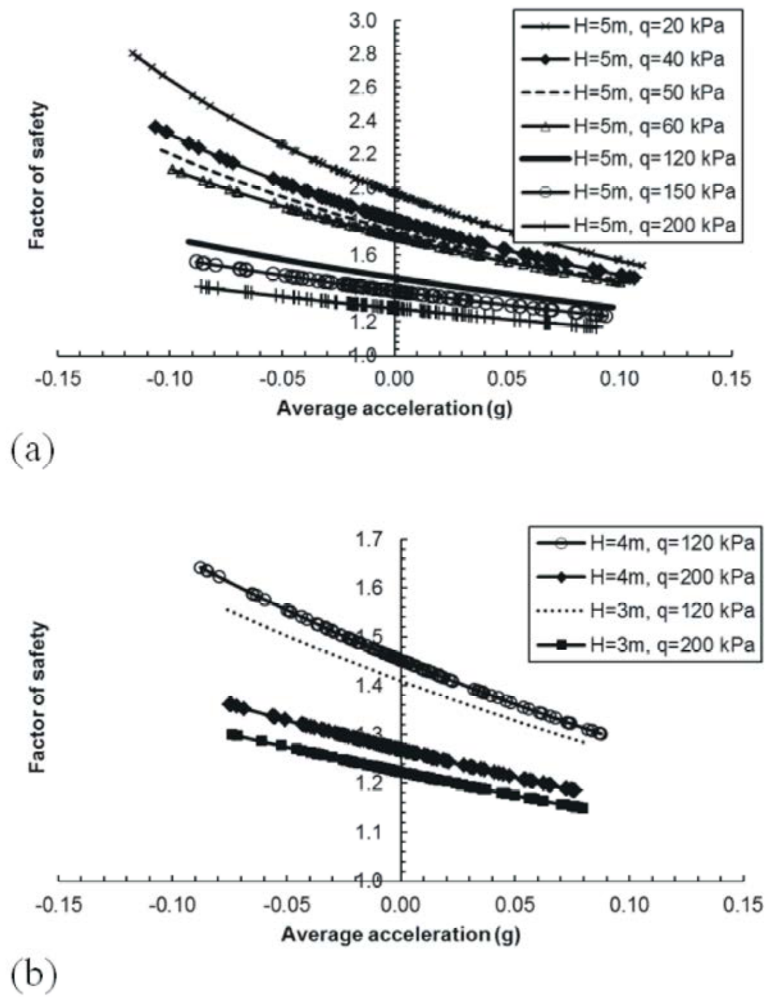

Fig. 8: Factor of safety versus average acceleration for: (a) slopes with height of 5m and (b) slopes with heights of 4m and 3m (peak base acceleration = 0.07g)

Therefore, a positive average acceleration is a downslope acceleration that promotes failure and contributes to the downslope permanent seismic deformation. On the other side, a negative average acceleration is in the upslope direction and, hence, may cause an upslope stabilizing deformation.

It is proposed in this study to define the threshold acceleration marking the onset of permanent seismic deformation development inside the slope. The proposed definition is based on the premise that plastic deformations do not only occur when the factor of safety drops below unity, but they are initiated, even locally, at safety factors above unity. The proposed threshold acceleration is calculated such that the permanent seismic deformation calculated from the numerical analysis matches the permanent seismic deformation calculated by double integrating the acceleration records in excess of the threshold acceleration.

The numerical analyses results indicate that the toe displacement is negligible relative to the crest displacement. In addition, the displacement troughs shown in Figure 5 indicate that the displacement drops significantly at a distance of about 2.0-3.0 meters from the slope crest. These results show that the crest displacement can be considered a direct indicator of the overall slope deformation.

A trial and error procedure with a simple spreadsheet is implemented to estimate the permanent seismic deformation using the proposed modified Newmark/Chopra approach. The procedure is summarized as follows:

- An arbitrary value of the threshold acceleration is assumed. The arbitrary value is positive, because negative accelerations do not cause downslope deformations.
- The average acceleration time history is truncated at the proposed threshold acceleration and the following rules apply:
    - If the average acceleration at a certain time is greater than the assumed threshold acceleration, the assumed threshold acceleration is subtracted from the average acceleration and the difference is double integrated to calculate the permanent seismic deformation.
    - If the acceleration at a certain time is equal to or smaller than the assumed threshold acceleration, the permanent seismic deformation is considered zero.
- Using the simple trapezoidal numerical integration rule, the modified acceleration time history is integrated to obtain the incremental velocity during each time interval. Hence, the total velocity is calculated.
- The velocity record is integrated to obtain the displacement record.
- The calculated displacement time history is compared with the finite-element-based time history (numerical approach).
- Different values of the threshold acceleration are tried and the numerical integration calculations are repeated until a practical match is achieved.

The results are shown in detail for the case of the 5m-high slope loaded with a surcharge of 120 kPa (peak base acceleration = 0.07g). The average acceleration time history is shown above in Figure 7. After few trials, the threshold acceleration that provides the best practical match with the finite element results equals 0.059g. Figure 9 shows the truncated acceleration time history where accelerations equal to or smaller than the threshold acceleration are considered zero. Figure 10 shows the velocity time history and Figure 11 shows the displacement time history. Figure 11 shows also the displacement time history calculated by the finite element procedure. The numerical-based deformation matches the value based on the proposed threshold acceleration.

The threshold acceleration of the 5m-high slope loaded with a surcharge of 120 kPa (0.059g) corresponds to a factor of safety of 1.353 (see Figure 8). The static factor of safety equals 1.464; i.e. the threshold acceleration value corresponds to a factor of safety 92.4% of the static value.

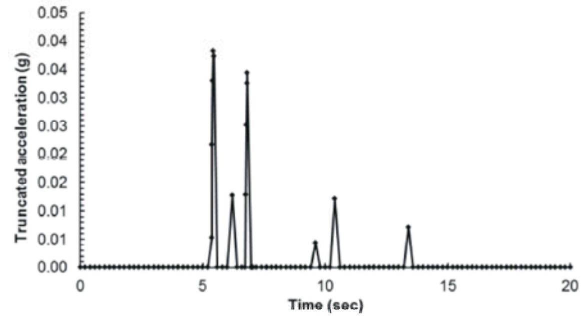

Fig. 9: Truncated average acceleration time history for a threshold acceleration of 0.059g for the 5m-high slope with surcharge 120 kPa (peak base acceleration = 0.07g)

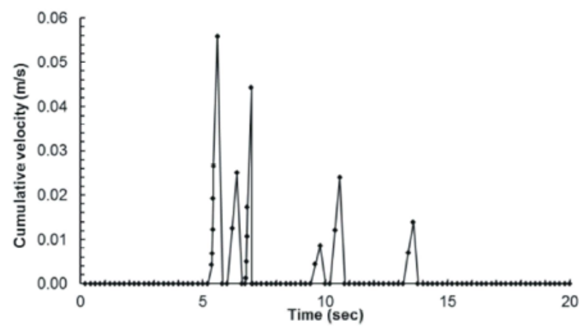

Fig. 10: Calculated velocity time history for H=5m and q=120 kPa (peak base acceleration = 0.07g)

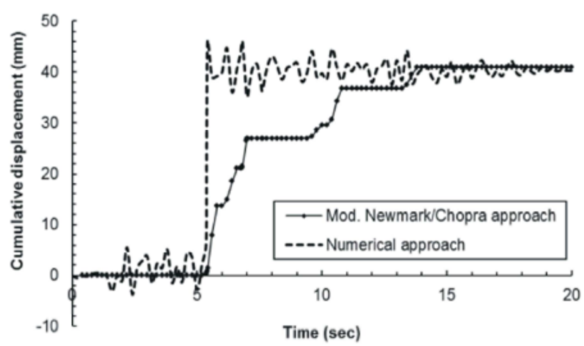

Fig. 11: Calculated displacement time history from modified Newmark/Chopra approach and from the numerical approach for H=5m and q=120 kPa (peak base acceleration = 0.07g)

The same procedure is followed for the other slope configurations. Figure 12 through Figure 17 show the calculated permanent seismic deformation records for some cases using the numerical approach and the proposed modified Newmark/Chopra approach (peak base acceleration = 0.07g). The displacement time histories calculated by the two approaches are in good agreement especially towards the end of the seismic excitation.

Table 2: Summary of results (peak base acceleration = 0.07g)

H (m), q (kPa)	FS_{static}	Threshold acceleration, a_s (g)	FS at a_s	Threshold acceleration ratio [FS_{as} / FS_{static}] (%)
5, 20	1.968	0.079	1.635	83.1
5, 40	1.808	0.079	1.540	85.2
5, 50	1.746	0.075	1.510	86.5
5, 60	1.710	0.066	1.518	88.8
5, 120	1.464	0.059	1.353	92.4
5, 150	1.384	0.054	1.296	93.6
5, 200	1.280	0.049	1.217	95.0
4, 120	1.452	0.069	1.331	91.6
4, 200	1.268	0.053	1.210	95.4
3, 120	1.410	0.065	1.306	92.6
3, 200	1.222	0.057	1.168	95.6

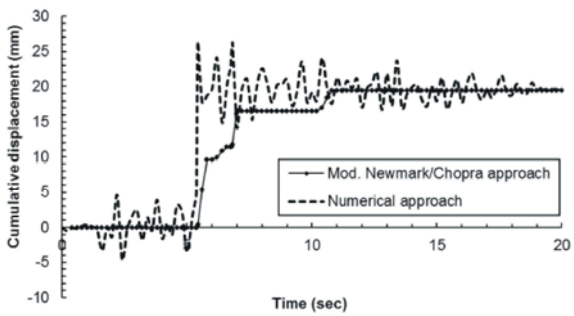

Fig. 12: Calculated displacement time history from modified Newmark/Chopra approach and from the numerical approach for H=5m and q=60 kPa (peak base acceleration = 0.07g)

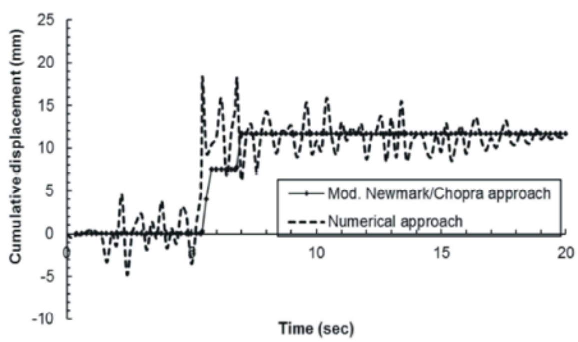

Fig. 13: Calculated displacement time history from modified Newmark/Chopra approach and from the numerical approach for H=5m and q=50 kPa (peak base acceleration = 0.07g)

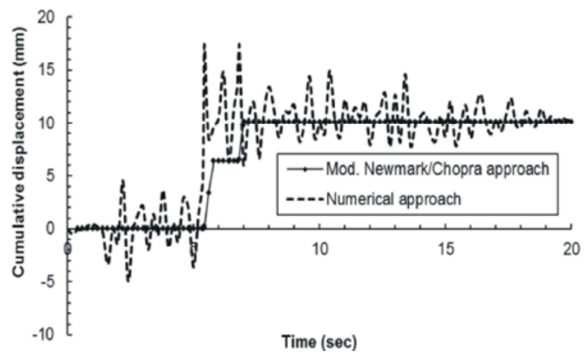

Fig. 14: Calculated displacement time history from modified Newmark/Chopra approach and from the numerical approach for H=5m and q=40 kPa (peak base acceleration = 0.07g)

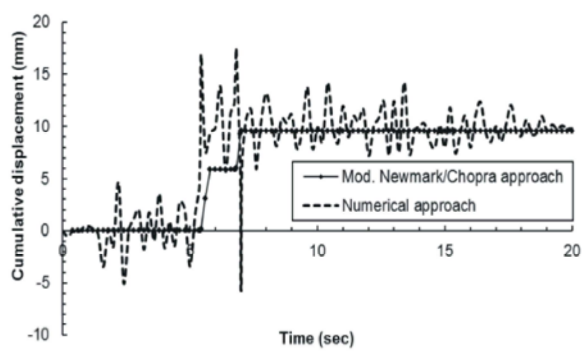

Fig. 15: Calculated displacement time history from modified Newmark/Chopra approach and from the numerical approach for H=5m and q=20 kPa (peak base acceleration = 0.07g)

The eleven cases shown in Table 1 are investigated under a peak base acceleration of 0.07g. Table 2 summarizes the values of the threshold acceleration, the corresponding factor of safety, the static factor of safety and the "threshold acceleration ratio". The threshold acceleration ratio is defined as the factor of safety corresponding to the threshold acceleration divided by the static factor of safety. Based on the results shown in Table 2, the relation between the applied surcharge and the threshold acceleration ratio is plotted in Figure 18. The results show that, for the same input motion intensity, the slope height has a minor effect on the threshold acceleration ratio. The applied surcharge is the main influencing factor for same soil parameters.

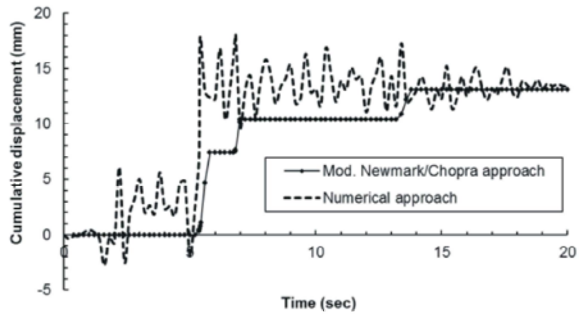

Fig. 16: Calculated displacement time history from modified Newmark/Chopra approach and from the numerical approach for H=4m and q=120 kPa (peak base acceleration = 0.07g)

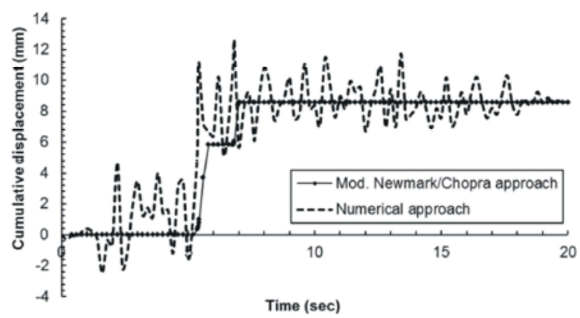

Fig. 17: Calculated displacement time history from modified Newmark/Chopra approach and from the numerical approach for H=3m and q=120 kPa (peak base acceleration = 0.07g)

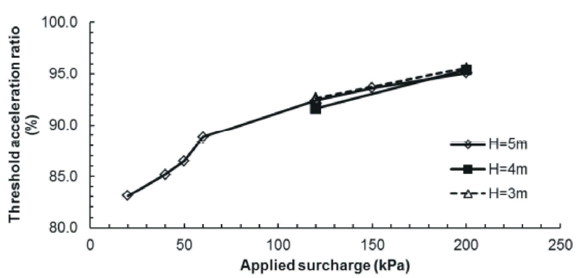

Fig. 18: Threshold acceleration ratio versus applied surcharge (peak base acceleration = 0.07g)

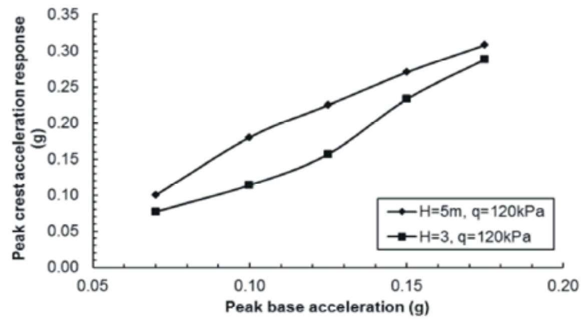

Fig. 19: Peak crest acceleration versus peak base acceleration for 3 and 5m-high slopes loaded with 120 kPa

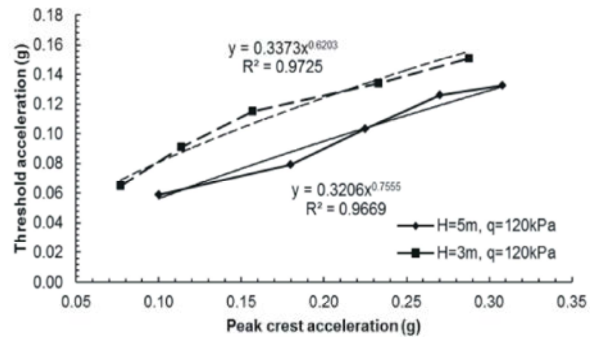

Fig. 20: Threshold acceleration versus peak crest acceleration for 3 and 5m-high slopes loaded with 120 kPa

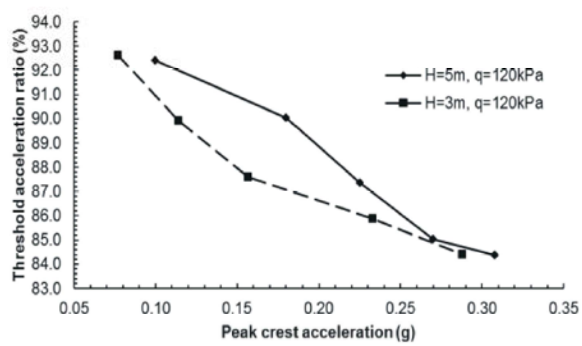

Fig. 21: Threshold acceleration ratio versus the peak crest acceleration for 3 and 5m-high slopes loaded with 120 kPa

The effect of the peak input acceleration is also investigated. Peak base accelerations of 0.10g, 0.125g, 0.15g and 0.175g are investigated for the 3.0 and 5.0 m-high slopes loaded with a surcharge of 120 kPa, in addition to the base case of peak input acceleration of 0.07g. The results are interpreted in terms of the effect of the peak crest acceleration on the threshold acceleration and the threshold acceleration ratio. The interpretation of the results in terms of the peak crest acceleration rather than the peak base acceleration allows for excluding the effects of waves' magnification/attenuation. Figure 19 shows the relationship between the peak input acceleration and the peak crest acceleration. Figure 20 shows the relationship between the threshold acceleration and the peak crest acceleration for the 3.0 and 5.0 m-high slopes. Both relationships fit to a power function. Figure 21 shows the effect of the peak crest acceleration on the threshold acceleration ratio.

DISCUSSION

The results indicate that Newmark [1] model and Chopra [2] modifications cannot be used to estimate the permanent seismic deformation of finite slopes with the classical definition of the yield acceleration. A factor of safety of unity is required for the complete development of a well-defined shear surface. However, permanent seismic deformations start to accumulate with the initiation of local yield zones inside the soil mass. The analyses conducted in this paper show that the permanent seismic deformation of dry sand slopes starts to accumulate at a threshold acceleration ratio ranging from 83% to 96%, i.e. at factors of safety of 83-96% of the static values. Higher threshold acceleration ratios result from weaker seismic excitation with relatively higher surcharge values (peak base acceleration of 0.07g and a surcharge of 120-200 kPa). By increasing the intensity of the input motion to 0.175g, the threshold acceleration ratio drops to 84%. Smaller surface surcharges, e.g. 20 kPa, cause the threshold acceleration ratio to drop also to 83%. The deduced range of the threshold acceleration ratio can be used to determine upper and lower bounds of the permanent seismic deformation.

The analyses conducted at the same peak base acceleration of 0.07g indicate that the slope height has a minimal effect on the threshold acceleration ratio (see Figure 18). The applied surcharge has the most influencing effect for the same soil properties. For the range of stresses expected from footings on slopes, i.e. 120-200 kPa, the threshold acceleration ratio ranges from 92% to 96% at this level of seismic excitation, which indicates that the match between Newmark/Chopra approach and the numerical approach can be achieved at safety factors closer to the static value than to unity.

The investigation of the effect of the earthquake intensity on the threshold acceleration shows that the threshold acceleration can be correlated with the peak crest acceleration through a power function, as shown in Figure 20. The interpretation of the results in terms of the crest response eliminates the effect of the waves' magnification/attenuation through the soil mass. The power correlation can be written in the following general form:

$$a_s = (m.(a_{crest})^n \quad (3)$$

where a_s is the threshold acceleration (g), a_{crest} is the peak crest acceleration (g) and m and n are coefficients that reflect the effects of the slope height, the applied surcharge and the soil properties. The values of the coefficients m and n are shown in Figure 20.

The proposed threshold acceleration is different from Newmark's yield acceleration. The threshold acceleration marks the onset of the development of local yield zones inside the soil mass due to the exceedance of the soil strength by the seismic shear stresses. Hence, the proposed threshold acceleration marks the onset of the permanent seismic deformation development. On the other side, Newmark's yield acceleration corresponds to a factor of safety of unity and, hence, it marks the development of a complete well-defined sliding surface.

CONCLUSIONS

The conclusions of the study can be summarized in the following points:

- Permanent seismic deformations of finite dry sand slopes during earthquakes are initiated at safety factors greater than unity.
- A simplified approach is proposed to determine the threshold acceleration above which permanent seismic deformations start to develop inside the slope. The proposed threshold acceleration is obtained by conducting a seismic finite element analysis and a limit equilibrium analysis at each time step during the earthquake.
- The proposed threshold acceleration corresponds to a range of the factor of safety of 83-96% of the static factor of safety. This range can be used to estimate upper and lower bounds of the permanent seismic deformation of dry sand slopes.
- The threshold acceleration is correlated with the peak crest acceleration using a power law.
- The proposed procedure may overcome the difficulties associated with numerical analysis like convergence and solution time. However, the numerical approach is still more powerful in capturing local yielding and upslope deformations.

ACKNOWLEDGMENTS

The author would like to thank Professor Mohamed N. Fayed for his support.

REFERENCES

1. Newmark, N.M., 1965. Effects of earthquakes on dams and embankments. Géotechnique, 15(2): 139-160.

2. Chopra, A.K., 1966. Earthquake effects on dams. Ph.D. thesis, University of California, Berekely.
3. Elgamal, A.W., R.F. Scott, M.F. Succarieh and L. Yan, 1990. La Villita dam response during five earthquakes including permanent deformation. J. Geotech. Engrg., 116(10): 1443-1462.
4. Mateo, E.R., 2009. Seismic analysis and instrumentation of the Patillas Earth Dam. M.Sc. thesis, University of Puerto Rico, Mayaguez campus.
5. Du, W., 2013. Earthquake-induced slope displacement analysis using spatially-correlated vector intensity measures. Ph.D. thesis, Hong Kong University of Science and Technology.
6. Zangeneh, N., 2003. Enhanced Newmark method for seismic analysis of submarine slopes. M.Eng. Report, Memorial University of Newfoundland, Canada.
7. Wartman, J., 1999. Physical model studies of seismically induced deformations in slopes. Ph.D. thesis, University of California, Berkeley.
8. Law, K.T., K. Refahi, P. Ko, T. Lam and P. Hassan, 2005. Seismic Deformation of Waba Dam. Conference Proceeding: Canadian Dam Association, Calgary, Alberta, Canada.
9. Finn, W.D.L., M. Yogendrakumar, R.C. Lo and N. Yoshida, 1988. Direct computation of permanent seismic deformations. Proc. 9th World Conference on Earthquake Engineering, VIII: 219-224.
10. US Beareau of Reclamation. Seismic Risks for Embankments. 2012. URL: http://www.usbr.gov/ssle/damsafety/Risk/BestPractices/27-SeismicEmbankment20121207.pdf (last accessed December 2015).
11. Kourkoulis, R., I. Anastasopoulos, F. Gelagoti and G. Gazetas, 2010. Interaction of foundation-structure systems with seismically precarious slopes: Numerical analysis with strain softening constitutive model. Soil Dynamic and Earthquake Engineering, 30: 1430-1445.
12. GEO-SLOPE International Ltd. Stress-Deformation Modeling with SIGMA/W 2007. Third Edition, March 2008.
13. GEO-SLOPE International Ltd. Dynamic Modeling with QUAKE/W 2007. Third Edition, March 2008.
14. GEO-SLOPE International Ltd. Stability Modeling with SLOPE/W 2007. Third Edition, March 2008.
15. Janbu, J., 1963. Soil compressibility as determined by Oedometer and triaxial tests. in: Proc. of 3rd European Conference on Soil Mechanics and Foundation Engineering, Wiesbaden, 1: 19-25.
16. Seed, H.B. and I.M. Idriss, 1970. Soil moduli and damping factors for dynamic response analyses. Report EERC 70-10, Earthquake Engineering Research Center, University of California, Berkeley.
17. Ishibashi, I and X. Zhang, 1993. Unified dynamic shear moduli and damping ratios of sand and clay. Soils and Foundations, 33(1): 182-191.
18. Abdel-Motaal, M.A., 1999. Soil effect on the dynamic behavior of framed structures, Ph.D. Thesis, Ain Shams University, Egypt.
19. Mokhtar, A.A., M.A. Abdel-Motaal and M.M. Wahidy, 2014. Lateral displacement and pile instability due to soil liquefaction using numerical model. Ain Shams Engineering Journal, 5(4): 1019-1032.